NASA TECHNICAL NOTE

NASA TN D-5276

NASA TN D-5276

TRIM ATTITUDE, LIFT AND DRAG OF THE APOLLO COMMAND MODULE WITH OFFSET CENTER-OF-GRAVITY POSITIONS AT MACH NUMBERS TO 29

by Charles E. DeRose

Ames Research Center
Moffett Field, Calif.

NATIONAL AERONAUTICS AND SPACE ADMINISTRATION • WASHINGTON, D. C. • JUNE 1969

NASA TN D-5276

TRIM ATTITUDE, LIFT AND DRAG OF THE APOLLO COMMAND MODULE WITH OFFSET CENTER-OF-GRAVITY POSITIONS AT MACH NUMBERS TO 29

By Charles E. DeRose

Ames Research Center
Moffett Field, Calif.

NATIONAL AERONAUTICS AND SPACE ADMINISTRATION

For sale by the Clearinghouse for Federal Scientific and Technical Information
Springfield, Virginia 22151 – CFSTI price $3.00

TRIM ATTITUDE, LIFT AND DRAG OF THE APOLLO COMMAND MODULE WITH OFFSET CENTER-OF-GRAVITY POSITIONS AT MACH NUMBERS TO 29

By Charles E. DeRose

Ames Research Center

SUMMARY

Measurements have been made with free-flight test models of the drag, lift, and trim attitude of a shortened version of the Apollo Command Module for Mach numbers 10 to 29 and free-stream Reynolds numbers 20,000 to 300,000. The tests were performed in the Ames Hypervelocity Free-Flight Aerodynamic Facility, using models launched from a 1.27-cm bore light-gas gun. Two center-of-gravity positions (offset from the model centerline by 0.046 and 0.028 diameter) were investigated. Resulting trim angles were 151° and 162°, respectively. Lift/drag ratios for the two trim angles were 0.435 and 0.255. Both trim angle and lift/drag ratio showed no variation with Mach number or Reynolds number within the limits investigated.

Lift and drag data obtained from this investigation compare quite closely to those obtained from previous wind-tunnel tests and from Apollo flight results. Good agreement of the trim angles was obtained when, in each case, the location of the center of gravity was referenced to the axis of symmetry of the primary pressure supporting surface, the blunt face.

INTRODUCTION

The Apollo Spacecraft Program has been supported by a test program involving many research and industrial test facilities of the country. A vast quantity of basic stability characteristics of the Apollo Command Module have already been determined; much of this information is condensed and summarized in reference 1. These data are for a smooth-faced, symmetrical model with and without antennas, fairings, and proturberances, for Mach numbers 0.2 to 18.

Of particular interest for this configuration is the determination of values of trim angle and lift/drag ratio at trim as a function of the displacement of the center of gravity (cg) from the model centerline. These values of trim angle and lift/drag ratio are available from various wind-tunnel tests up to Mach number 18 and form a consistent set of results. However, this is far below the anticipated Mach number of 35 for the entering Apollo on the lunar return.

To fill the void between Mach numbers 18 and 35, a high-speed, free-flight test program (ref. 2) was undertaken. The results of that test, made with models with no offset of the cg, and flying with the heat shield forward, indicated that the drag, and hence the trim angle, of a model with an offset cg, may vary with Mach number above about 20.

In addition, data at low Reynolds numbers at Mach number 14 (ref. 3) indicated a reduction of lift/drag ratio at a specific trim angle and an increase in trim angle for a given offset cg position with reductions in free-stream Reynolds numbers below 8000. Also, flight tests (ref. 4) of the Apollo Command Module with the design nonsmooth heat shield, gave trim angles that consistently differed from wind-tunnel results by 3° to 4°.

Because of the above results, it was decided to measure the trim angle and lift/drag ratio of a trimmed Apollo model over the range of velocities and Mach numbers in which there was doubt as to the values of these quantities. (This investigation was not extended to a low Reynolds number range because of facility limitations.) The measurements were made in the Ames Hypervelocity Free-Flight Aerodynamic Facility using 0.95-cm-diameter models with two displaced cg positions. Velocities were varied from 3.5 to 7.3 km/sec and Mach numbers from 10 to 29. To attain these velocities, the models were gun-launched through both still air and counterflow airstreams.

SYMBOLS

C_D	drag coefficient, $\frac{D}{qS}$, dimensionless
C_L	lift coefficient, $\frac{L}{qS}$, dimensionless
C_{L_α}	lift-curve slope, $\frac{\partial C_L}{\partial \alpha}$, per radian
$C_{L_{\alpha^3}}$	nonlinear portion of lift-curve slope, $\frac{\partial C_L}{\partial \alpha^3}$, per radian^3
cg	center of gravity
D	drag force, N
d	reference diameter, maximum diameter of model, m
K_1, K_2, K_3	constants in equation for tricyclic motion (eq. (1))
L	lift force, N
M	Mach number

m	model mass, kg
p	model roll rate, used in equation (1)
q	dynamic pressure $[(1/2\rho_\infty U^2]$, N/m^2
Re	Reynolds number, based on model diameter and free-stream conditions
rms	root mean square
S	reference area, $\frac{\pi d^2}{4}$, m^2
t	time, sec
U	total model velocity, m/sec
X,Y,Z	orthogonal tunnel-fixed reference axes, X axis horizontal and positive in the flight direction, Z positive downward
X',Y',Z'	model principal axes
X_{cg}	normal distance from line tangent to front face of model to cg, m
Z_{cg}	perpendicular distance from reference centerline to cg, m
α	angle of attack (in XZ plane), radians
α_r	resultant angle of attack, radians
α_{rms}	root-mean-square resultant angle of attack, $\pi - \left[\frac{1}{X}\int_o^X (\pi - \alpha_r)^2 \, dX\right]^{1/2}$, radians, deg in figures
α_{trim}	trim angle of attack, radians, deg in figures
β	angle of sideslip (in XY plane), radians
n_1,n_2	damping exponents (eq. (1))
φ	angle of roll (in YZ plane), radians
ρ_∞	free-stream air density, kg/m^3
ω_1,ω_2	rates of rotation of vectors that describe the model oscillatory motion in equation (1)

Subscripts

r resultant, denotes terms in plane of the resultant angle of attack

o at time zero

y terms in the XY plane

z terms in the XZ plane

Superscripts

($\dot{}$) first derivative with respect to time

($\ddot{}$) second derivative with respect to time

FACILITY

The Ames Hypervelocity Free-Flight Aerodynamic Facility is a shock-tube-driven, blow-down-type wind tunnel, which produces a counterflow airstream for an instrumented ballistic range. Figure 1 is a sketch of this facility. The 23-m-long test section has 16 orthogonal pairs of photographic stations spaced 1.5 m apart. Details of the operating cycle of this facility are similar to those discussed for a prototype facility in reference 5.

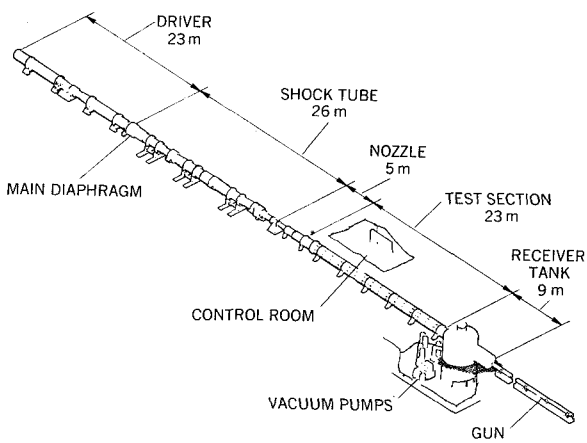

Figure 1.- Hypervelocity free-flight aerodynamic facility.

Figure 2 is a line sketch of the facility and loading pressures for the counterflow tests. One feature, not described in reference 5, was added for the counterflow portion of this test. The dump tank was separated from the test section by a set of plastic diaphragms and was maintained at a pressure of 35 torr (T), whereas the pressure in the test section was nominally 0.3 T prior to airflow. This relatively high pressure in the dump tank made it possible to use aerodynamic forces to separate the sabot halves from the model. The diaphragms were removed by the starting shock wave in the test section before the arrival of the model so that they had no adverse effect on the test model. The high pressure in the dump tank did not affect the flow in the test section until well after the model flight was completed. For still-air testing, all diaphragms were eliminated except the blowoff diaphragm, and the shock tube was replaced with a model catcher.

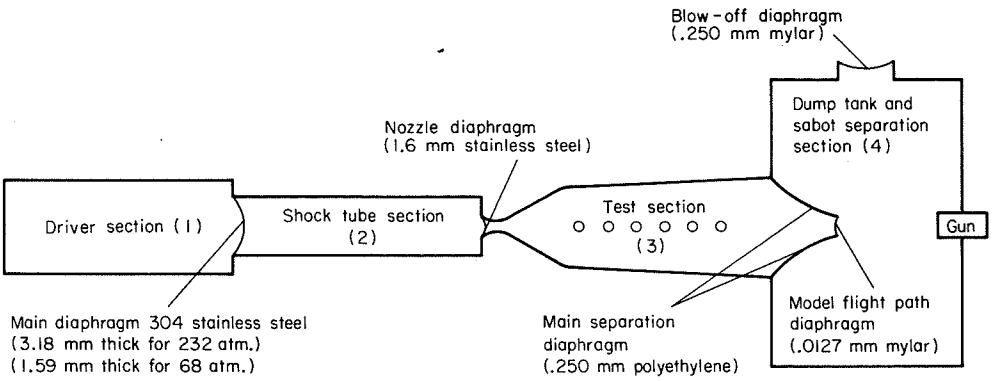

Nominal counterflow loading conditions

Combustion drive U_∞ = 2.9 km/sec T_∞ = 410° K			
Driver section (1) 33 atm. load 232 atm. after burn (Helium 12.4 atm.) (Hydrogen 8.2 atm.) (Air 12.2 atm.) (Oxygen .2 atm.)	Shock tube (2) .74 atm. air Shock-wave Mach number = 5.7	Test section (3) .0004 atm. air p_∞ = .02 atm.	Dump tank (4) .046 atm. air
Cold helium and air drive U_∞ = 1.4 km/sec T_∞ = 100° K			
Driver section (1) 68 atm. load (Helium 57 atm.) (Air 11 atm.)	Shock tube (2) 1.94 atm. air Shock-wave Mach number = 2.6	Test section (3) .0004 atm. air p_∞ = .01 atm.	Dump tank (4) .046 atm. air

Figure 2.- Hypervelocity free-flight facility arrangement for counterflow testing.

For this test program, the launch gun was a 1.27-cm-diameter light-gas gun of the type described in reference 6. The ultimate launch velocity reached was approximately 4800 m/sec, a figure dictated by sabot and model limitations rather than by gun capability.

Three different airstreams were used to span the ranges of Mach numbers and Reynolds numbers. Still air (i.e., with no counterflow) was used for the Mach number 10 to 14 results. A Mach number 7 airstream of 2900 m/sec velocity was used to obtain the Mach number 17 and 18 data. This airstream was produced by a helium-hydrogen-oxygen combustion drive, moderated by the addition of nitrogen. The Mach number 26 to 29 data were obtained by flying the model through a Mach number 7, 1400 m/sec counterflow airstream. This airstream was produced by an air-diluted, cold helium drive. Loading pressures for the two counterflows are shown in figure 2.

Photographic data of the time history of the model flight attitude and position were obtained from the 16 pairs of orthogonal shadowgraph stations, each of which was spark illuminated and Kerr-cell shuttered to produce an exposure time of 30 ns. The timing information was recorded by 16 100-MHz counters activated by signals from the Kerr-cell shutters. Sample shadowgraphs are shown in figure 3.

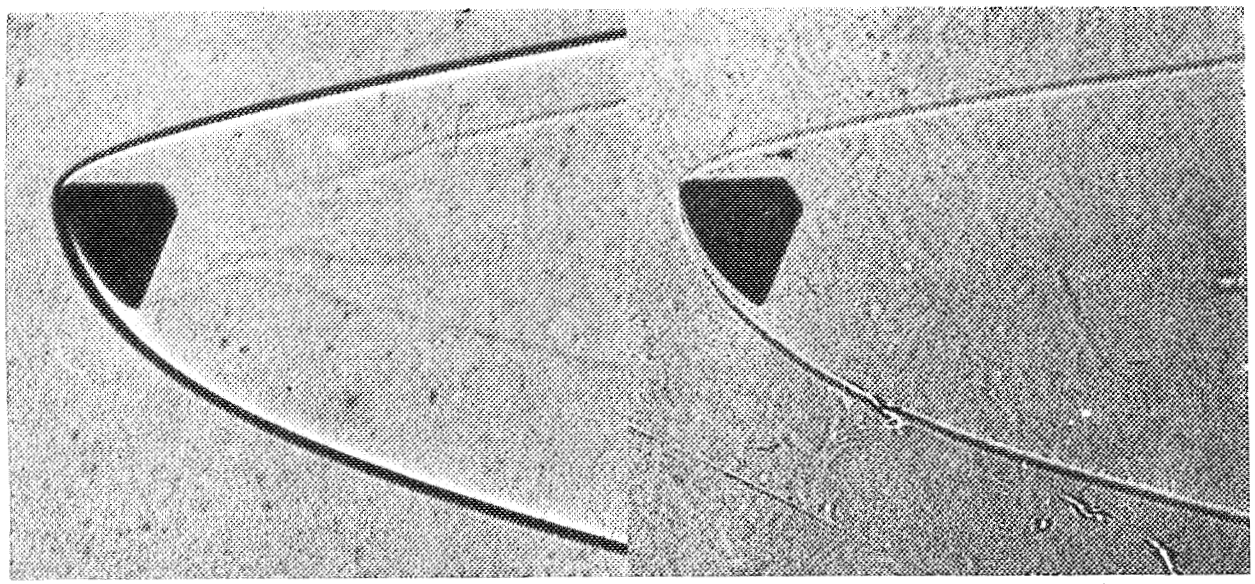

(a) Mach number 10.2, Reynolds number 214,000, velocity 3.52 km/sec.

(b) Mach number 17.0, Reynolds number 52,500, velocity 6.60 km/sec.

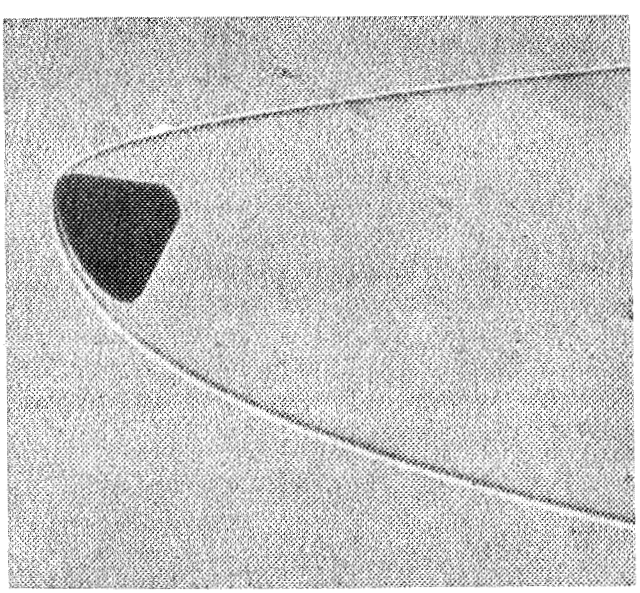

(c) Mach number 26.4, Reynolds number 160,900, velocity 5.30 km/sec.

Figure 3.- Shadowgraphs of Apollo model in flight

MODELS AND SABOTS

Figure 4 is a sketch of a typical model used for this test program. The shortening of the model (a modification to permit convenient positioning of the cg) represents a change in shape of the actual Apollo Command Module. This modification is not expected to have any effect on the high-speed aerodynamic characteristics of interest in this investigation because of the small surface area removed. The models were constructed of steel to obtain a high density, which minimized the model's swerve.

The cg was shifted off the centerline with pressed-in slugs of high and low density materials. For a Z_{cg}/d of -0.046, a transverse slug of sintered tungsten alloy (specific gravity 16.8) was used on the top, and a vertical slug of magnesium (specific gravity 1.8) was used on the bottom as shown in figure 4. For a Z_{cg}/d of -0.028, only the magnesium slug was used.

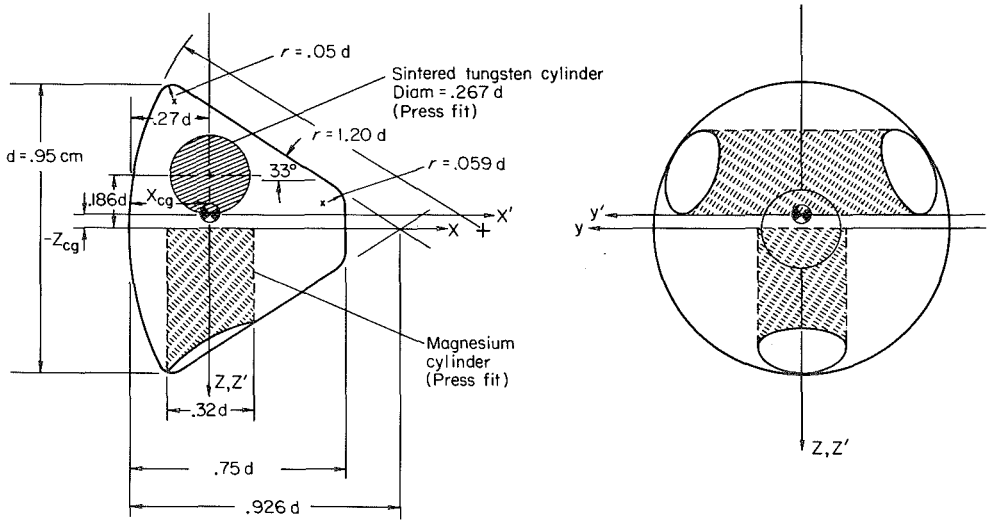

Figure 4.- Free-flight model.

A sabot used to launch the models is shown in figure 5. The models were held at the anticipated trim angle in a two-piece split polycarbonate cylinder. Each model was secured in the sabot with small tabs, which were formed from the sabot wall by using a hot iron. To prevent propellant gas from impinging on the models, seals of polyester film were placed directly behind the sabot.

The cg position of the models was measured very accurately because the test data are sensitive to its location. A change of 0.0015 in Z_{cg}/d theoretically produces a 1° change in the trim angle of attack. For the scale of models used for this test this represents 0.014 mm in Z_{cg}. The cg positions were measured independently by two persons, each of whom made two or more measurements to minimize errors in cg determination. The

average value of all the measurements was used. The variation was approximately ±0.005 mm. On the basis of this error band in the determination of the cg position, the maximum error in trim angle of attack from this source is believed to be ±0.3°.

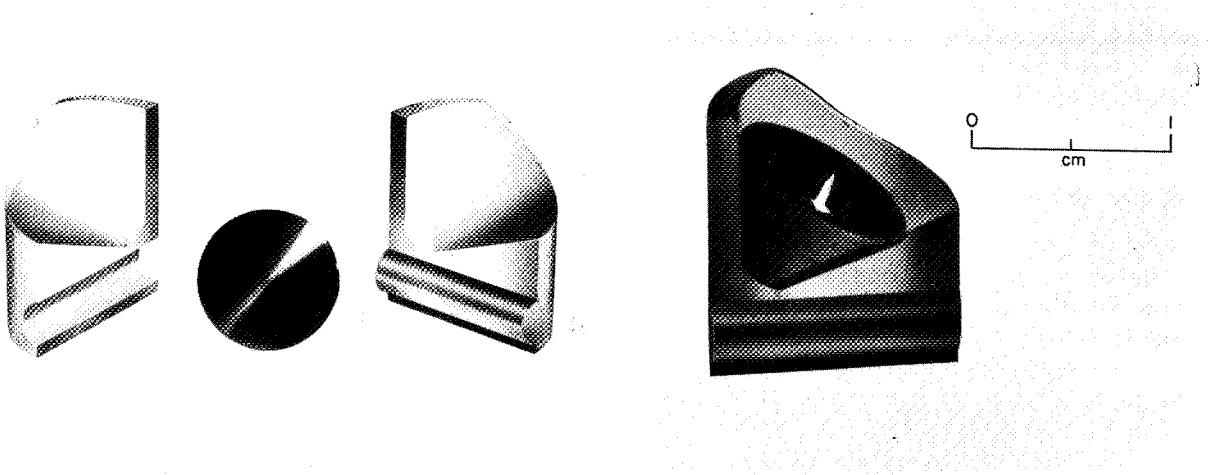

Figure 5.- Model and sabot.

The models were machined, with form tools carefully ground to match the contours shown in figure 4. Figure 6 shows profile measurements made from enlarged photographs of four models and the computed profile. The accuracy of reproduction indicates that all models represent one configuration.

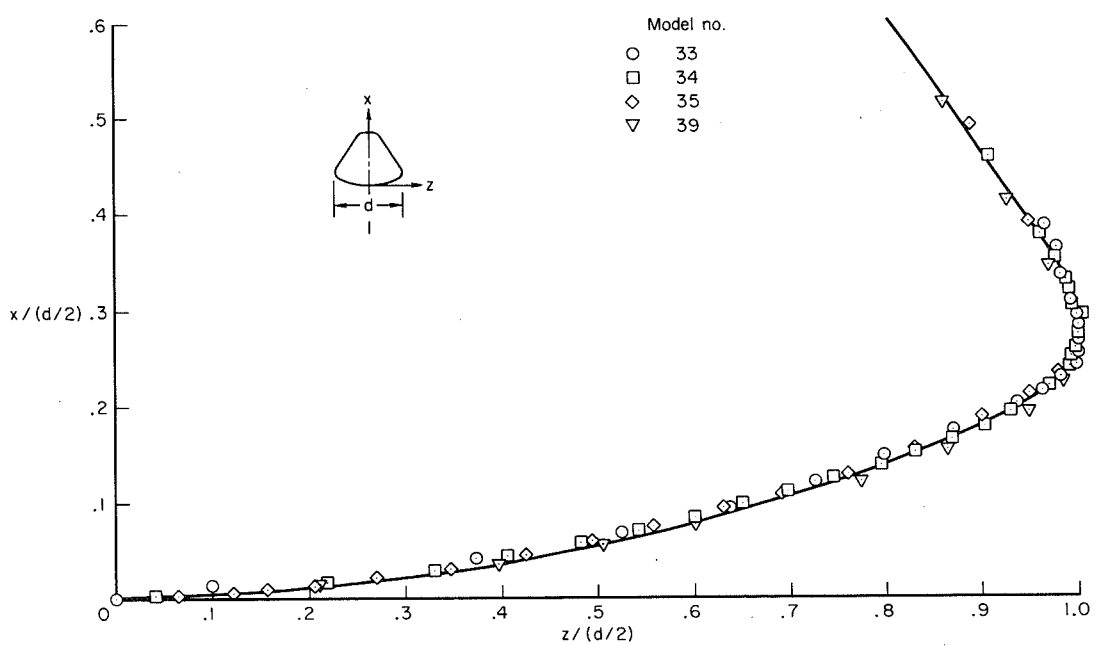

Figure 6.- Measurements of model profile coordinates.

DATA REDUCTION

The models were launched at their anticipated trim angle so that the trim attitude could be measured without the analysis of large amplitude oscillations. With a low disturbance launch, a model would fly at its trim angle with small residual pitching and yawing oscillations. The initial orientation of the model X'Z' plane, the plane of trim angle of attack, was usually located 45° off the tunnel-fixed XZ plane so that a maximum model swerve could be accommodated. Figure 7 shows the model-fixed and tunnel-fixed axes systems and the angle definitions.

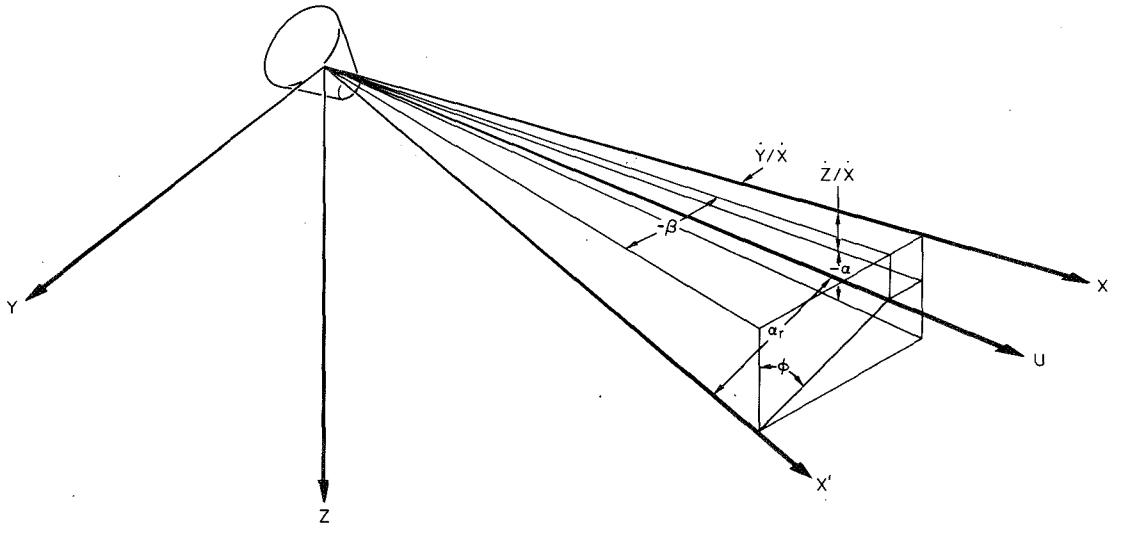

Figure 7.- Axes and angle definitions.

The basic method of obtaining the trim angles of attack was to fit the distance history of the model's angular motion with the equation for tricyclic motion:

$$\beta + i\alpha = K_1 e^{(\eta_1 + i\omega_1)X} + K_2 e^{(\eta_2 - i\omega_2)X} + K_3 e^{ipX} \qquad (1)$$

where K_3 is the trim angle. A full description of this data analysis can be found in reference 7.

It must be noted that the nature of this test violated some of the simplifying assumptions of the tricyclic motion equation; for example, the model was not axisymmetric (inertial) and had large trim angles and nonlinear aerodynamics. However, since this method was used only to obtain the trim angle, it is believed that the procedure was justified. Graphical procedures were used on flights showing no roll so that the values produced by the above method could be checked. The results produced by both methods agreed within ±1/2°.

The lift coefficient was determined by an independent method (discussed below) from measurements of the time history of model cg position and is represented as a linear plus cubic function of angle of attack.

$$C_L = C_{L_\alpha}\alpha + C_{L_{\alpha^3}}\alpha^3 \tag{2}$$

The time histories of the component angles were converted into a time history of the resultant angle of attack.

$$\alpha_r \approx \tan^{-1}(\tan^2\alpha + \tan^2\beta)^{1/2} \tag{3}$$

This approximation is exact when the swerves ($\dot{Y}/\dot{X}$ and $\dot{Z}/\dot{X}$) are zero. Negligible errors were introduced by swerves of the magnitude observed for these flights (maximum value observed was 0.008 radian). The lift force in the plane of the resultant angle of attack was then written

$$L_r = \left(C_{L_\alpha}\alpha_r + C_{L_{\alpha^3}}\alpha_r^3\right)(qS) \tag{4}$$

This plane of the resultant angle of attack can be defined by the roll angle φ, where

$$\tan\varphi \approx \frac{\tan\beta}{\tan\alpha} \tag{5}$$

This is assumed to be an exact expression because of the small swerve corrections. Then the component of the lift force in the Z direction can be expressed as

$$L_z = C_{L_\alpha}(qS)(\alpha_r\cos\varphi) + C_{L_{\alpha^3}}(qS)(\alpha_r^3\cos\varphi) \tag{6}$$

and the component in the Y direction can be expressed as

$$L_y = C_{L_\alpha}(qS)(\alpha_r\sin\varphi) + C_{L_{\alpha^3}}(qS)(\alpha_r^3\sin\varphi) \tag{7}$$

Then if the gravity term in the XZ plane is ignored

$$L_z = m\ddot{Z} \quad \text{and} \quad L_y = m\ddot{Y} \tag{8}$$

where

$$\ddot{Z} = C_{L_\alpha}\left(\frac{qS}{m}\right)\alpha_r\cos\varphi + C_{L_{\alpha^3}}\left(\frac{qS}{m}\right)\alpha_r^3\cos\varphi \tag{9}$$

$$\ddot{Y} = C_{L_\alpha}\left(\frac{qS}{m}\right)\alpha_r\sin\varphi + C_{L_{\alpha^3}}\left(\frac{qS}{m}\right)\alpha_r^3\sin\varphi \tag{10}$$

Although the models did decelerate a measurable amount, the velocity was assumed constant during each flight to facilitate evaluating the lift. Thus, integrated twice with respect to time, equations (9) and (10) become:

$$Z_t - Z_o = \dot{Z}_o t + C_{L_\alpha}\left(\frac{qS}{m}\right)\int_o^t\int_o^t \alpha_r \cos\varphi \, dt \, dt + C_{L_{\alpha^3}}\left(\frac{qS}{m}\right)\int_o^t\int_o^t \alpha_r{}^3 \cos\varphi \, dt \, dt \tag{11}$$

$$Y_t - Y_o = \dot{Y}_o t + C_{L_\alpha}\left(\frac{qS}{m}\right)\int_o^t\int_o^t \alpha_r \sin\varphi \, dt \, dt + C_{L_{\alpha^3}}\left(\frac{qS}{m}\right)\int_o^t\int_o^t \alpha_r{}^3 \sin\varphi \, dt \, dt \tag{12}$$

The unknown constants ($\dot{Z}_o$, $\dot{Y}_o$, C_{L_α}, and $C_{L_{\alpha^3}}$) were computed by the method of least squares applied to equations (11) and (12) at each station. While it is true that a continuous time history of α_r and φ would be desirable in the evaluation of the double integrals, data were obtained at a sufficient number of photographic stations during each flight to evaluate the double integrals using Gauss' formula for numerical integration.

Drag coefficients were obtained from the deceleration of the model and calculated by the method of reference 8. Sufficient drag measurements were obtained from the several model flights to give an accurate variation of drag coefficient with rms resultant angle of attack. This variation of drag coefficient, together with the value of C_L computed from each flight, was used to obtain the trim lift/drag ratio.

ACCURACY

The accuracy of the free-flight data was controlled by the precision with which the test conditions and model attitude could be measured. This accuracy is estimated below:

ρ_∞	M = 10-14	±0.2 percent
	M = 17-18, 26-29	±3.0 percent
M		±0.1 percent
α, β		±0.25°

The computed results are estimated to have the following uncertainty:

α_{trim}		±1°
C_D	M = 10-14	±0.02
	M = 17-18, 26-29	±0.05
L/D		±0.025

RESULTS AND DISCUSSION

All results are shown in graphical form in figures 8 through 12 for the flights listed in table I. The data are compared with wind-tunnel results from references 1 and 9 and with Apollo flight data from reference 4.

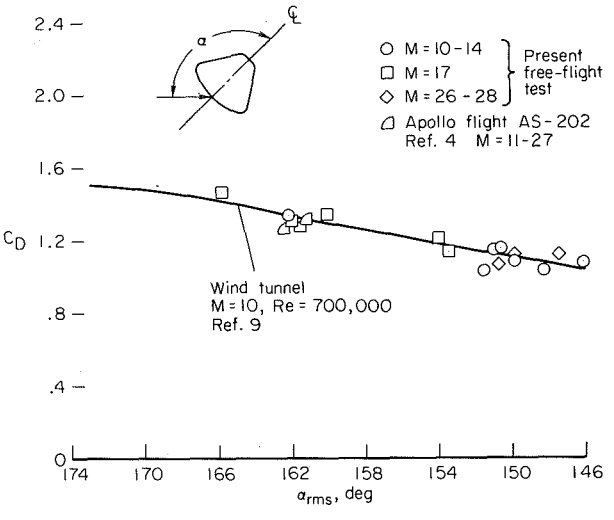

Figure 8.- Drag coefficient as function of angle of attack.

Drag

Drag coefficient as a function of rms resultant angle of attack is presented in figure 8. As the models were flying essentially backward (blunt face forward), the angles measured in these free-flight tests were (180 - α_r). The root mean squares of these angles were computed and then subtracted from 180° to give the angles consistent with previous Apollo tests. The data points for the three Mach number ranges tested are identified by symbol notation. The present free-flight data agree closely with both the wind-tunnel and the Apollo full-scale flight results, and there is no discernible variation of drag coefficient with Mach number or Reynolds number for the test conditions.

Trim Angle

Figure 9 shows values of trim angle as a function of the cg offset (Z_{cg}/d) for the three Mach number ranges of the present test and for the data of references 1 and 4. All trim angles shown were adjusted to a common axial cg position ($X_{cg}/d = 0.270$). The adjustments to the free-flight results amounted to less than 0.4° in the most severe case. In agreement with the results of references 1 and 4, Mach number apparently had no effect on the trim angles achieved in the present test.

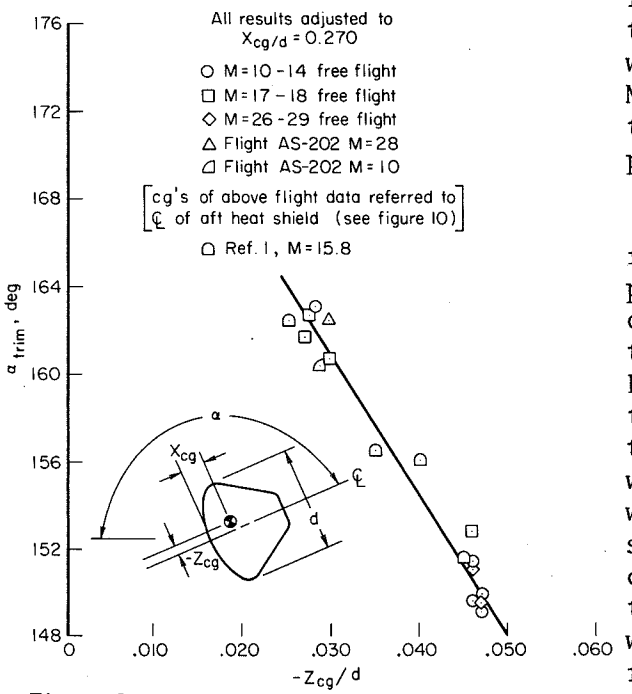

Figure 9.- Trim angle as function of center-of-gravity displacement.

It should be noted that the data from reference 4 are plotted at cg positions measured from the centerline of the blunt-face heat shield rather than from the structural centerline. Figure 10 shows the cg with respect to the structural and heat-shield centerlines. The heat-shield centerline was used to reference the cg because, when flying heat shield forward, this surface supports the significant aerodynamic forces and, therefore, appears the more logical choice. For example, with the heat-shield centerline as the reference, at $\alpha = 180°$ and no cg offset, the pitching moment would be

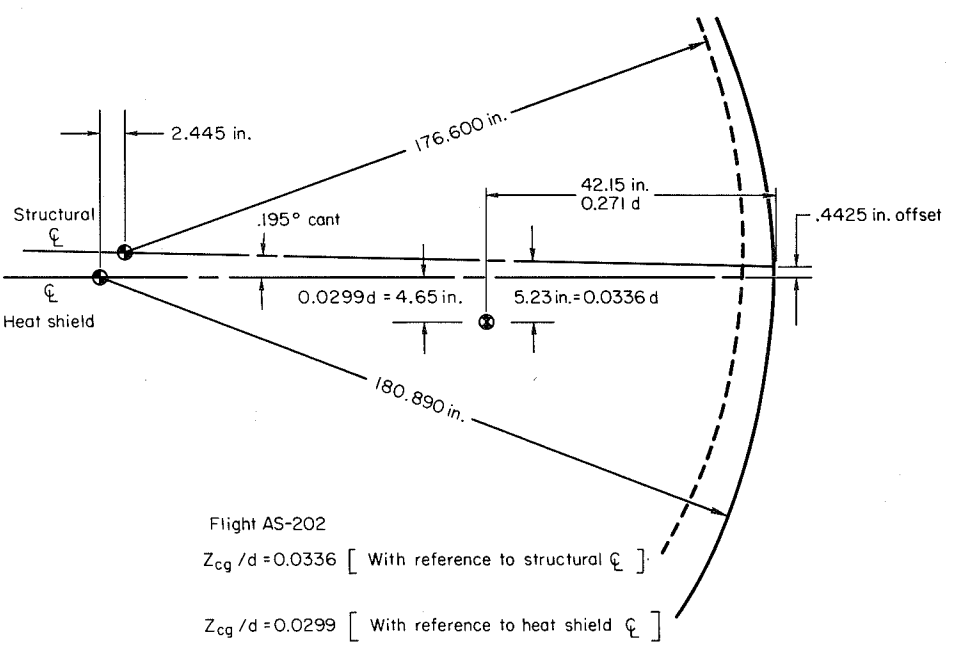

Figure 10.- Comparison of asymmetric configuration's structural and heat-shield centerlines.

essentially zero and the configuration trimmed. As seen in figure 9, using the heat-shield centerline to locate the cg provides a good correlation of the flight data of reference 4 with the present free-flight data and earlier wind-tunnel data. Earlier correlations of flight and wind-tunnel trim angles (refs. 4 and 10) were not successful because the structural centerline of the Apollo Command Module was used to locate its cg. The heat-shield centerline is the only consistent reference that can be used when symmetrical Apollo configurations are compared with those having unsymmetrical heat shields.

Lift Coefficient

Lift coefficients obtained from flights with trim angles of about 150° and 160° are shown in figure 11 as a function of angle of attack. Each curve covers the angle-of-attack range measured for that flight. Also shown are wind-tunnel results from reference 9 obtained at a Mach number of 10 and a Reynolds number of 700,000. The present results for resultant trim angles of 150° (fig. 11(a)) agree well with each other and with the wind-tunnel data except near the maximum value of C_L. Because of the higher angles and lower lift coefficients produced in the flights shown in figure 11(b), the lift is assumed to be only a linear function of the angle of attack. The slope and the values of C_L at angles of attack close to 160° agree well with both the wind-tunnel results and the curves of figure 11(a).

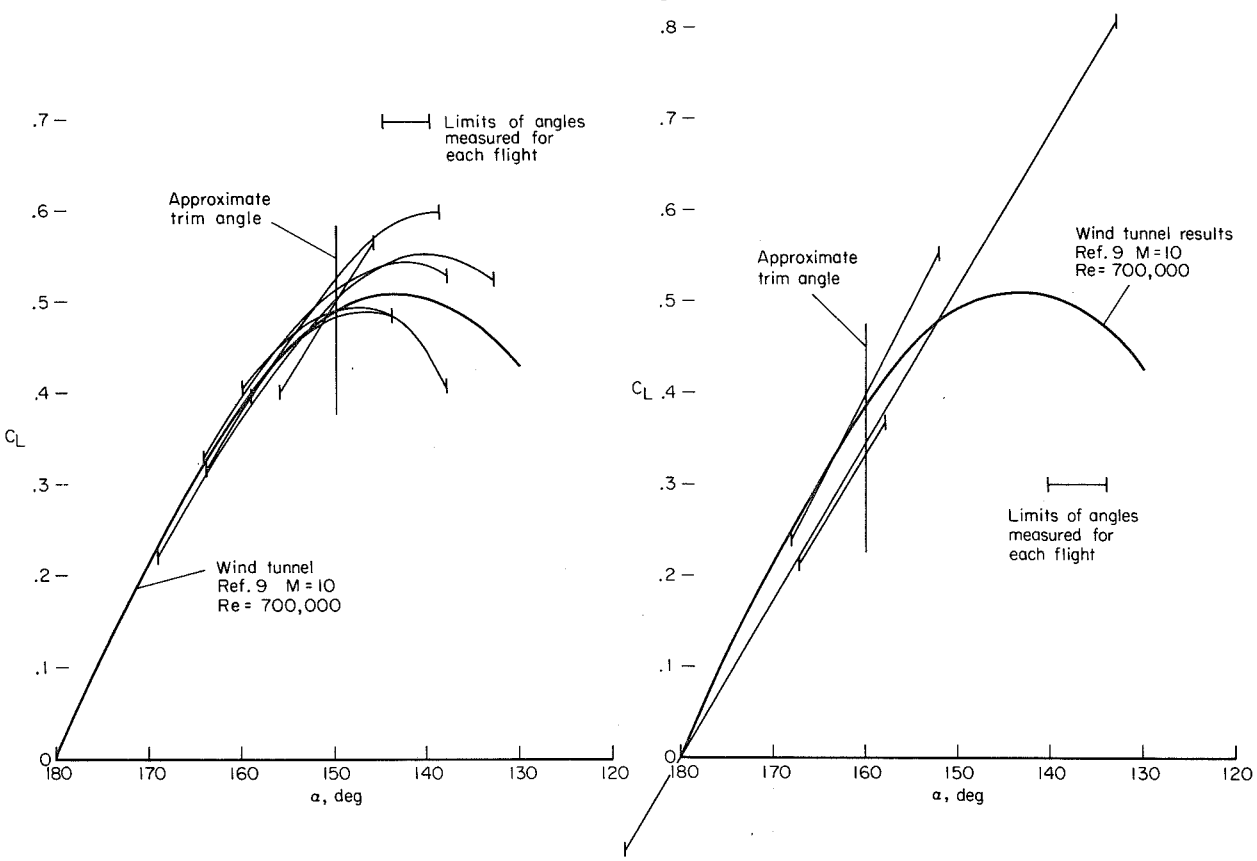

(a) Lift measured for models trimmed nominally at 150°.

(b) Lift measured for models trimmed nominally at 160°.

Figure 11.- Lift coefficient versus angle of attack.

Lift/Drag Ratio

Figure 12 shows values of lift/drag ratio as a function of trim angle of attack. The free-flight results compare quite well with values obtained from wind-tunnel tests (refs. 1 and 9) and from Apollo flight tests (ref. 4). The free-flight data show no effect of Mach number or Reynolds number.

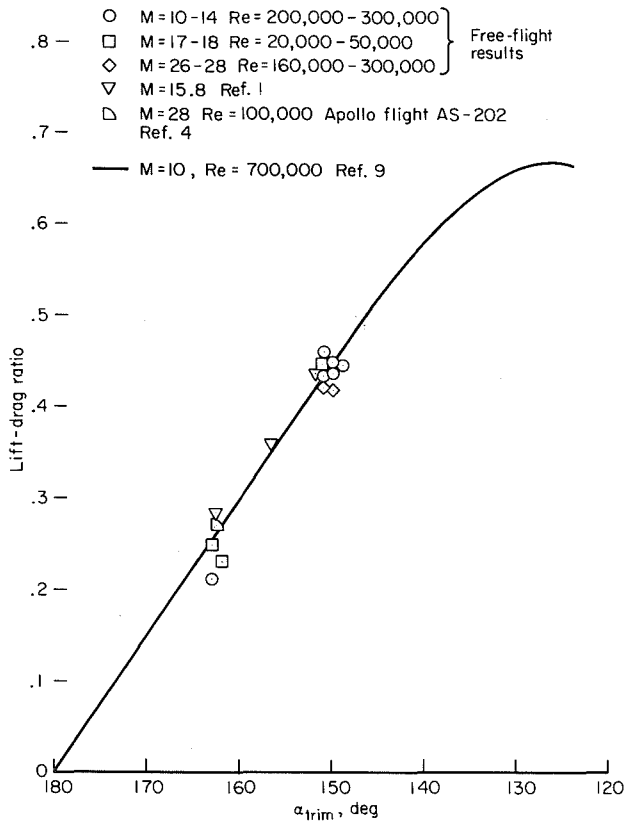

Figure 12.- Lift-drag ratio as functions of trim angle of attack.

CONCLUSIONS

The lift, drag, and trim angles of the Apollo Command Module show no indication of being affected by either Mach number or Reynolds number in the range tested, which extends from Mach numbers 10 to 29 and Reynolds numbers 20,000 to 300,000 (based on free-stream conditions and body diameter). The lift and drag agree closely with previous wind-tunnel results and full-scale flight results. The trim angles likewise agree closely when, in each case, the center-of-gravity offset is related to the axis of symmetry of the primary pressure supporting surface, the blunt face.

Ames Research Center
National Aeronautics and Space Administration
Moffett Field, Calif. 94035 Mar. 10, 1969
124-07-02-18-00-21

REFERENCES

1. Moseley, William C., Jr.; Moore, Robert H., Jr.; and Hughes, Jack E.: Stability Characteristics of the Apollo Command Module. NASA TN D-3890, 1967.

2. Sammonds, Robert I.: Forces and Moments on an Apollo Model in Air at Mach Numbers to 35 and Effects of Changing Face and Corner Radii. NASA TM X-1086, 1965.

3. Horstmann, C. C.; and Kussoy, M. I.: Free-Flight Measurements of Aerodynamic Viscous Effects on Lifting Re-entry Bodies. AIAA Paper 67-165.

4. Hillje, Ernest R.: Entry Flight Aerodynamics From Apollo Mission AS-202. NASA TN D-4185, 1967.

5. Seiff, Alvin: Ames Hypervelocity Free-Flight Research. Astronautics and Aerospace Engineering, vol. 1, no. 11, Dec. 1963, pp. 16-23.

6. Curtis, John S.: An Accelerated Reservoir Light Gas Gun. NASA TN D-1144, 1962.

7. Malcolm, Gerald N.; and Chapman, Gary T.: A Computer Program for Systematically Analyzing Free Flight Data to Determine the Aerodynamics of Axisymmetric Bodies. NASA TN D-4766, 1968.

8. Seiff, Alvin: A New Method for Computing Drag Coefficients From Ballistic Range Data. J. Aero. Sci., vol. 25, no. 2, Feb. 1958, pp. 133-134.

9. Staff of von Karman Gas Dynamics Facility, AEDC: Data Report for Apollo Model FS-3 Wind Tunnel Tests in Tunnels Band C of the AEDC von Karman Gas Dynamics Facility. Dec. 10, 1962 (Contract NAS9-150).

10. Griffith, B. J.; and Boylan, D. E.: Reynolds and Mach Number Simulation of Apollo and Gemini Re-Entry and Comparison With Flight. ARO, Inc. AGARD Conference Proceedings No. 30 (preprint), Hypersonic Boundary Layers and Flow Fields, May 1968.

TABLE I.- FREE-FLIGHT TEST CONDITIONS AND RESULTS

Run number	Mach number	Velocity, u_∞, km/sec	Reynolds number, $\frac{\rho_\infty u_\infty d}{\mu_\infty}$	Free-stream temp., °K	X_{cg}/d	Z_{cg}/d	α trim, deg	Angular range of oscilla-tion, deg	C_D	α rms, deg	L/D at 151°	L/D at 162°
1512	11.15	3.86	306,180	290	0.2771	0.0458	151	162-140	1.076	146.2	---	---
41	10.28	3.55	217,510	290	.2743	.0471	150	156-146	1.161	150.6	0.43	---
47	10.17	3.51	214,200	290	.2770	.0460	---	164-139	1.077	149.9	.46	---
63	17.01	6.60	52,547	378	.2712	.0499	---	164-138	1.136	153.5	.45	---
159	11.14	3.85	235,180	290	.2719	.0462	150	159-144	1.145	151	.43	---
161	12.76	4.41	215,020	290	.2760	.0478	---	169-133	1.030	151.5	.44	---
162	13.95	4.80	236,570	290	.2748	.0469	149	160-138	1.033	148.3	.43	---
200	26.43	5.30	160,910	100	.2740	.0467	149	158-144	1.064	150.7	.42	---
239	28.96	5.78	293,570	100	.2719	.0459	151	157-139	1.117	147.5	---	---
240	28.61	5.72	306,330	100	.2693	.0471	---	155-144	1.116	150.0	.42	---
242	17.99	7.21	22,205	410	.2729	.0458	153	159-138	1.214	154.0	---	---
248	17.86	7.16	19,225	410	.2750	.0297	161	178-143	1.465	165.8	---	---
286	17.92	7.23	27,570	405	.2750	.0274	163	168-152	1.341	160.1	---	0.27
290	17.53	7.17	24,760	405	.2730	.0271	162	186-133	---	152.2	---	.23
291	13.70	4.68	291,000	290	.2700	.0281	163	167-158	1.338	162.2	---	.24

NATIONAL AERONAUTICS AND SPACE ADMINISTRATION
WASHINGTON, D. C. 20546

OFFICIAL BUSINESS

FIRST CLASS MAIL

POSTAGE AND FEES PAID
NATIONAL AERONAUTICS AND
SPACE ADMINISTRATION

POSTMASTER: If Undeliverable (Section 158 Postal Manual) Do Not Return

"The aeronautical and space activities of the United States shall be conducted so as to contribute . . . to the expansion of human knowledge of phenomena in the atmosphere and space. The Administration shall provide for the widest practicable and appropriate dissemination of information concerning its activities and the results thereof."

—NATIONAL AERONAUTICS AND SPACE ACT OF 1958

NASA SCIENTIFIC AND TECHNICAL PUBLICATIONS

TECHNICAL REPORTS: Scientific and technical information considered important, complete, and a lasting contribution to existing knowledge.

TECHNICAL NOTES: Information less broad in scope but nevertheless of importance as a contribution to existing knowledge.

TECHNICAL MEMORANDUMS: Information receiving limited distribution because of preliminary data, security classification, or other reasons.

CONTRACTOR REPORTS: Scientific and technical information generated under a NASA contract or grant and considered an important contribution to existing knowledge.

TECHNICAL TRANSLATIONS: Information published in a foreign language considered to merit NASA distribution in English.

SPECIAL PUBLICATIONS: Information derived from or of value to NASA activities. Publications include conference proceedings, monographs, data compilations, handbooks, sourcebooks, and special bibliographies.

TECHNOLOGY UTILIZATION PUBLICATIONS: Information on technology used by NASA that may be of particular interest in commercial and other non-aerospace applications. Publications include Tech Briefs, Technology Utilization Reports and Notes, and Technology Surveys.

Details on the availability of these publications may be obtained from:

SCIENTIFIC AND TECHNICAL INFORMATION DIVISION

NATIONAL AERONAUTICS AND SPACE ADMINISTRATION

Washington, D.C. 20546